

UNIVERSIDADE DE SÃO PAULO

**INSTITUTO DE FÍSICA
CAIXA POSTAL 20516
01498 - SÃO PAULO - SP
BRASIL**

PUBLICAÇÕES

IFUSP/P-867



**A QUANTITATIVE ANALYSIS OF INSTABILITIES IN
THE LINEAR CHIRAL SIGMA MODEL**

M.C. Nemes, M. Nielsen and M.M. de Oliveira
Instituto de Física, Universidade de São Paulo

J. da Providência
Centro de Física Teórica (INIC), Universidade de Coimbra
P-3000 Coimbra, Portugal

Agosto/1990

A QUANTITATIVE ANALYSIS OF INSTABILITIES IN THE LINEAR CHIRAL SIGMA MODEL

M.C. NEMES, M. NIELSEN and M.M. de OLIVEIRA

Instituto de Física, Universidade de São Paulo, Caixa Postal 20516 - 01498 São Paulo,
Brazil

J. da PROVIDÊNCIA¹

Centro de Física Teórica (INIC), Universidade de Coimbra, P-3000 Coimbra, Portugal

Abstract: We present a method to construct a complete set of stationary states corresponding to small amplitude motion which naturally includes the continuum solution. The energy weighted sum rule (EWSR) is shown to provide for a quantitative criterium on the importance of instabilities which is known to occur in nonasymptotically free theories. Our results for the linear σ model showed be valid for a large class of models. A unified description of baryon and meson properties in terms of the linear σ model is also given.

1. INTRODUCTION

One of the main open problems in the area of particle physics nowadays is the understanding of the properties of hadrons starting from the microscopic theory of strong interactions, namely quantum chromodynamics (QCD). The most powerful although technically very involved methods to treat this nonabelian gauge theory rely on Monte Carlo lattice calculations. In spite of being very complicated and sometimes not at all transparent, these calculations may serve as a guiding factor when one uses simplified phenomenological models. There have also been various theoretical attempts [1-6] to derive such models starting from QCD. One has been able to arrive at chiral effective meson and quark-meson lagrangians. In using such simplified models, however, one has to be very careful and make sure that the results are not very sensitive to their high energy behaviour, which is known to deviate radically from the behaviour of QCD. As pointed out by Perry and Cohen et al. [7], the break down of such theories happen when the momentum scale greatly exceeds other mass scales in the problem. In such regions one can not rely upon theoretical results which ignore the internal structure of nucleons and mesons.

The main characteristics of QCD which should be incorporated in phenomenological models to describe hadrons are essentially three: confinement, chiral symmetry and asymptotic freedom. The first two have been incorporated in a variety of models. The low energy spectra of hadrons have been successfully described by some of these models, namely the MIT bag model [8] or its generalizations which includes chiral symmetry [9] or still by topological soliton models [10]. As to what concerns asymptotic freedom, there is a rigorous result which states that phenomenological models lacking such property will present instabilities. Not as much work has been devoted to this topic, i.e., to a quantitative study of the importance of such instabilities.

The purpose of the present paper is twofold: Firstly to introduce a method to obtain a complete set of stationary states corresponding to small amplitude motion. The method stems from traditional many body techniques in which the continuum solutions are naturally included. When applied to, eg., the linear σ model it allows, in particular, for the calculation of the pion decay constant. An interesting result of our calculations in the context of this model is that the EWSR can be a useful tool in giving a quantitative criterium to study Perry's instabilities. Although we shall be working

¹supported by JNICT-PORTUGAL

in the particular σ model, the method is general and the above conclusion should be valid for all phenomenological models which include the same ingredients (a fermionic field coupled to several bosonic fields). Secondly, we study the bosonic spectroscopy for both bound states and resonances of the linear σ model, and compare it with corresponding results obtained in the context of the Nambu Jona-Lasinio (NJL) [11] model, which is known to give a fairly good description of light meson spectra [12-15]. We show that this model may also provide an adequate description of the bosonic sector, analogous to the one given by the NJL model. This suggests that the chiral σ model may provide a unified framework for the description of both the baryonic and mesonic sectors.

In section 2 we present the chiral σ model which will be described semiclassically in the sense that fermions are treated quantum mechanically whereas meson fields are treated classically. The counterterms added to the hamiltonian are needed to assure stability of the ground state [16]. The meson spectra are given in section 3 for bound states and in section 4 for the continuum. The mesons in the continuum show up as quark-antiquark ($q\bar{q}$) resonances with a certain spreading width. Despite of the fact that this spreading width has no relation with the width associated with the decay of the resonances [17], the position of the resonances can be compared to experiment. Finally in section 5 we present some conclusions.

2. THE CHIRAL MODEL

The σ model is a field theoretical model originally introduced by Gell - Mann and Lévy [18] as an example of a phenomenological model which realizes one important characteristic feature of QCD, chiral symmetry and partial conservation of the axial current. It involves a fermionic iso-doublet field of zero bare mass interacting with a triplet of pseudoscalar pions $\vec{\Psi}$ and a scalar field σ .

In the present section we present a semiclassical realization of the above mentioned model, and introduce the corresponding effective hamiltonian describing a system of N fermions occupying either positive or negative energy states, interacting with the classical fields corresponding to $\vec{\Psi}$ and σ . Our effective hamiltonian is written as

$$H = \sum_{j=1}^N [\vec{p}_j \cdot \vec{\alpha}_j + g\beta_j(\sigma(x_j) + i\gamma_5(j)\vec{r}_j \cdot \vec{\Psi}(x_j))]$$

$$\begin{aligned} & + \frac{1}{2} \int d^3x (\Pi_\sigma^2 + \vec{\nabla}\sigma \cdot \vec{\nabla}\sigma + \Pi_\Psi^2 + \sum_{i=1}^3 \vec{\nabla}\Psi_i \cdot \vec{\nabla}\Psi_i) - \frac{K}{4} \int d^3x (\sigma^2 - \Psi^2 - \sigma_0^2)^2 \\ & + 2\xi \int \frac{d^3p d^3x}{(2\pi)^3} \sqrt{p^2 + g^2(\sigma^2 + \Psi^2)} \Theta(\Lambda^2 - p^2) + \frac{\lambda - 1}{2} \int d^3x (\Pi_\sigma^2 + \Pi_\Psi^2), \end{aligned} \quad (2.1)$$

where $\vec{\alpha}$, β and γ_5 are the usual Dirac matrices, \vec{r} correspond to the matrices of the fundamental flavor representation $SU(2)$, Π_σ and Π_Ψ are the conjugate momentum associated with the classical fields σ and $\vec{\Psi}$ respectively. The coupling constant g and the constants K and σ_0 will be fixed in the calculations in order to attribute physically reasonable masses for quarks and mesons. The factor ξ stands for the degeneracy of the system and will be taken equal to six (we shall be considering three colours). The last two terms in eq.(2.1) are renormalization terms, which depend on a cutoff parameter Λ [16]. The second renormalization term which contains the parameter λ allows for the definition of the scalar meson mass in the vacuum. Note that our hamiltonian is adjusted to the configuration space spanned by $|\vec{p}| < \Lambda$ and is invariant under a chiral rotation in the γ_5 - isospin space. More precisely, the replacements

$$\beta \rightarrow \beta + i\vec{\epsilon} \cdot [\gamma_5 \vec{r}, \beta],$$

$$i\beta\gamma_5 \vec{r} \rightarrow i\beta\gamma_5 \vec{r} + i\epsilon_j [\gamma_5 \tau_j, i\beta\gamma_5 \vec{r}],$$

$$\sigma \rightarrow \sigma - 2\vec{\epsilon} \cdot \vec{\Psi},$$

$$\vec{\Psi} \rightarrow \vec{\Psi} + 2\vec{\epsilon} \sigma,$$

where $\vec{\epsilon}$ is an infinitesimal constant vector, leave the hamiltonian, including counterterms, invariant.

In what follows we shall be considering an extended system of fermions, which are treated quantum mechanically and interact with classical fields, as described above.

The ground state of the model is determined variationally within the family of Slater determinants $|\phi_0\rangle$, or equivalently, of density matrices ρ_0 obtained by occupying single-particle positive energy states with momentum lower than P_F and single-particle negative energy states with momentum lower than Λ ($\Lambda > P_F$). In quark homogeneous matter we can write

$$\rho_0 = \frac{1}{2} \left(I + \frac{\vec{p} \cdot \vec{\alpha} + \beta M^*}{\sqrt{p^2 + M^{*2}}} \right) \Theta(P_F^2 - p^2) + \frac{1}{2} \left(I - \frac{\vec{p} \cdot \vec{\alpha} + \beta M^*}{\sqrt{p^2 + M^{*2}}} \right) \Theta(\Lambda^2 - p^2). \quad (2.2)$$

Here M^* is a variational parameter, representing the quark mass, to be fixed by the usual energy minimization procedure. The ground state energy in such a state can be immediately calculated and is given by

$$E = 2\xi \sum_p' \left(\sqrt{p^2 + M^{*2}} + \frac{M^*(g\sigma - M^*)}{\sqrt{p^2 + M^{*2}}} \right) + \frac{\lambda\Omega}{2} (\Pi_\sigma^2 + \Pi_\psi^2) + \frac{K\Omega}{4} (\sigma^2 + \Psi^2 - \sigma_0^2)^2 + 2\xi \sum_{p < \Lambda} \sqrt{p^2 + g^2(\sigma^2 + \Psi^2)}, \quad (2.3)$$

where $\sum_p' = \sum_{p < P_F} - \sum_{p < \Lambda}$ and Ω is the normalization volume. Variations with respect to M^* , σ and Ψ in the static case give the following relations

$$M^* = g\sigma, \quad (2.4)$$

$$\frac{2\xi}{\Omega} \sum_p' \frac{g^2\sigma^2}{\sqrt{p^2 + g^2\sigma^2}} + K(\sigma^2 + \Psi^2 - \sigma_0^2)\sigma + \frac{2\xi}{\Omega} \sum_{p < \Lambda} \frac{g^2\sigma^2}{\sqrt{p^2 + g^2(\sigma^2 + \Psi^2)}} = 0, \quad (2.5)$$

$$K(\sigma^2 + \Psi^2 - \sigma_0^2)\Psi + \frac{2\xi}{\Omega} \sum_{p < \Lambda} \frac{g^2\Psi^2}{\sqrt{p^2 + g^2(\sigma^2 + \Psi^2)}} = 0. \quad (2.6)$$

In the limit $\Lambda \rightarrow \infty$ the only solution of eq. (2.6) is $\Psi_i = 0$. The corresponding energy density is

$$\frac{E}{\Omega} = \frac{2\xi}{\Omega} \sum_{p < P_F} \epsilon + \frac{K}{4g^4} (M^{*2} - g^2\sigma_0^2)^2, \quad (2.7)$$

where $g\sigma$ has been replaced by M^* . We also get the self consistency condition

$$\frac{K}{g^4} (M^{*2} - g^2\sigma_0^2)M^* = -\frac{2\xi M^*}{\Omega} \sum_{p < P_F} \frac{1}{\epsilon}, \quad (2.8)$$

where $\epsilon = \sqrt{p^2 + M^{*2}}$.

From eq. (2.8) we see that the vacuum state ($P_F = 0$) is characterized by $M^* = M = g\sigma_0$ which is the constituent quark mass. If we are dealing with extended quark matter ($P_F \neq 0$) this effective mass will change according to the self consistency condition eq.(2.8). This implies that the energy per volume will be a function of P_F (or the effective quark mass) for a fixed set of parameters K , σ_0 and g . In Fig. 1 we show the energy per unit volume, eq.(2.7), as a function of M^* for some values of P_F . For small values of P_F , there are only two solutions for eq. (2.8), one corresponding to $M^* = 0$ (which remains as a solution for any values of P_F), and one corresponding to $M^* \neq 0$ which is the

minimal energy solution. However, as P_F grows the situation changes and we come into a region where eq. (2.8) provides three solutions. One of them corresponds to a maximum of the energy and must be discarded, the other two solutions correspond to a local and an absolute minimum of the energy. If we keep increasing P_F we will obtain only the solution $M^* = 0$. The symmetry is restored at $P_F = P_{FC}$ for which the two minima are degenerate.

The energy per particle represented in Fig. 2, refers to the absolute minimum solution. The curve is continuous, in spite of the discontinuous behaviour of M^* which is represented in Fig. 3 as a function of P_F . The reason for this becomes clear from Fig. 1 observing that at the point where the discontinuity in M^* occurs, namely P_{FC} , the two minima are degenerate and from that point forward we have always $M^* = 0$. Note that the energy per particle exhibits a pronounced minimum at the Fermi momentum $P_F = 1.55 fm^{-1}$ (for the values of the parameters given in the figure).

It is also important to emphasize that the inclusion of the Dirac sea plays an essential role in insuring the stability of the vacuum against fluctuations of M^* [16].

3. SCALAR AND PSEUDOSCALAR MESONS SPECTRA FOR BOUND STATES

In this section we present the time evolution of small homogeneous excitations (carrying zero momentum) around equilibrium. In considering this, the last counterterm in eq. (2.1) is very important to guarantee that the scalar meson mass in the vacuum corresponds to its physical mass (or the mass we choose as physically reasonable).

The time evolution of a density matrix $\rho(t)$ corresponding to a Slater determinant slightly displaced from equilibrium can be written as

$$\rho(t) = e^{iS(t)} \rho_0 e^{-iS(t)}, \quad (3.1)$$

where $S(t)$ is a hermitian, one-body, time dependent operator. For small amplitude motion, it is sufficient to consider the effect of $S(t)$ up to second order. Obviously, due to the coupling terms in the hamiltonian (eq.(2.1)) there will also be fluctuations in the scalar and pseudoscalar classical fields, respectively $\delta\sigma$ and $\delta\Psi_i$, which are non vanishing and time dependent. Consistently we shall treat these terms only up to second order. In order to obtain the equations of motion and corresponding eigenfrequencies and eigenvectors we follow the method presented in ref. [14].

The lagrangian describing small amplitude oscillations around the equilibrium state is

$$L = \frac{i}{2} \text{tr}(\rho_0[S, \dot{S}]) - \frac{1}{2} \text{tr}(\rho_0[S, [h_0, S]]) - i \text{tr}(\rho_0[S, \delta h]) + \frac{\Omega}{2} \left(\frac{(\delta \dot{\sigma})^2}{\lambda} + \frac{(\delta \dot{\Psi}_i)^2}{\lambda} \right) - \frac{K\Omega}{2g^2} [(3M^{*2} - M^2)(\delta\sigma)^2 + (M^{*2} - M^2)(\delta\Psi_i)^2] - \xi g^2 \sum_{p < \Lambda} \left(\frac{p^2}{\epsilon^3} (\delta\sigma)^2 - \frac{1}{\epsilon} (\delta\Psi_i)^2 \right), \quad (3.2)$$

where $h_0, \delta h$ are given by

$$h_0 = \bar{p} \cdot \bar{\alpha} + \beta M^*, \quad (3.3)$$

$$\delta h = \beta g \delta\sigma + i g \beta \gamma_5 \vec{\tau} \cdot \delta \vec{\Psi}. \quad (3.4)$$

The generators of the scalar and pseudoscalar homogeneous excitations for zero momentum transfer are respectively given by

$$S_\sigma = \bar{p} \cdot \bar{\alpha} \Phi_1(p^2, t) + i \beta \bar{p} \cdot \bar{\alpha} \Phi_2(p^2, t), \quad (3.5)$$

$$S_\Psi = i \beta \gamma_5 \vec{\tau} \cdot \vec{S}_1(p^2, t) + \gamma_5 \vec{\tau} \cdot \vec{S}_2(p^2, t). \quad (3.6)$$

Inserting eq. (3.5) in eq. (3.2) leads to the following equations of motion

$$\ddot{\Phi}_2 + 2M^* \dot{\Phi}_1 = 0, \quad (3.7a)$$

$$M^* \dot{\Phi}_1 - 2\epsilon^2 \Phi_2 + g \delta\sigma = 0, \quad (3.7b)$$

$$\frac{\delta \ddot{\sigma}}{\lambda} + \frac{K}{g^2} (3M^{*2} - M^2) \delta\sigma + \frac{2\xi g^2 \delta\sigma}{\Omega} \sum_{p < \Lambda} \frac{p^2}{\epsilon^3} + \frac{4\xi g \Phi_2}{\Omega} \sum_p' \frac{p^2}{\epsilon^3} = 0. \quad (3.7c)$$

The eigenfrequencies and eigenmodes are now easily obtained from the above equations. For the eigenfrequencies we get the following dispersion relation, corresponding to the scalar mode

$$\frac{\omega_\sigma^2}{\lambda} = \frac{K}{g^2} (3M^{*2} - M^2) + \frac{2\xi g^2}{\Omega} \sum_{p < \Lambda} \frac{p^2}{\epsilon^3} + \frac{8\xi g^2}{\Omega} \sum_p' \frac{p^2}{\epsilon(4\epsilon^2 - \omega_\sigma^2)}. \quad (3.8)$$

When describing the vacuum state we should have $\omega_\sigma = m_\sigma$, the scalar meson mass. We choose $m_\sigma = 2M$ (the justification for this choice is the comparison with the results obtained for the same spectrum in the NJL model ref.[13,14]). This requirement fixes the relation between K and g^2 to be

$$\frac{K}{g^2} = 2, \quad (3.9)$$

and also determines the parameter λ :

$$\frac{1}{\lambda} = 1 - \frac{\xi g^2}{2\Omega} \sum_{p < \Lambda} \frac{1}{\epsilon_0^3}, \quad (3.10)$$

where $\epsilon_0 = \sqrt{p^2 + M^2}$. Finally, the dispersion relation for the scalar meson mass reads

$$\omega_\sigma^2 = 6M^{*2} - 2M^2 + \frac{\xi g^2}{2\Omega} \sum_{p < \Lambda} \left(\frac{4p^2}{\epsilon^3} + \frac{\omega_\sigma^2}{\epsilon_0^3} \right) + \frac{8\xi g^2}{\Omega} \sum_p' \frac{p^2}{\epsilon(4\epsilon^2 - \omega_\sigma^2)}. \quad (3.11)$$

There are [19] two types of solution of eq.(3.11). If $\omega_\sigma = \pm\omega_{\sigma z}, \omega_{\sigma z} < 2\epsilon_F$, there are two collective discrete modes (bound states). On the other hand, if $2\epsilon_F < \omega_\sigma < 2\epsilon_A$, there is a continuum of solutions which we will discuss in detail in section 4 for the pseudoscalar excitation.

This dispersion relation is independent of the cutoff parameter Λ in the limit $\Lambda \rightarrow \infty$, but if Λ is too large one imaginary root appears [16]. However for values of the cutoff below a given critical value, of the order of $2M$, all roots are real implying dynamical stability of the system. To work with a finite cutoff Λ corresponds to the suggestion of Cohen et al.[7] (see section 4). In any case, the collective frequencies of the discrete modes are not very sensitive to the value of the cutoff Λ , for $\Lambda > 2M$.

The discrete scalar mass spectrum is shown in Fig. 3 and exhibits a qualitative behaviour very similar to the one found in ref.[14] for the NJL model. The main difference is connected with the way in which chiral symmetry is restored in the two models: in the NJL model (see ref.[13], Fig. 5) chiral symmetry is restored in a continuous fashion as the quark density matter increases, whereas in the present model a discontinuous behaviour may occur (see Fig. 3). This qualitative difference can be reduced by a convenient choice of parameters. There remains however a small quantitative difference: whereas in the NJL model the scalar meson mass is always given by $\omega_\sigma = 2M^*$, this is not the case any more in the present model, although the difference is not too large as shown in Fig. 3.

The scalar RPA eigenmodes for the bound states are given by

$$\Phi_1^{(\pm)} = -\frac{\pm i g \omega_{\sigma z}}{M^*} \frac{\sigma^{(\pm)}}{4\epsilon^2 - \omega_{\sigma z}^2}, \quad (3.12a)$$

$$\Phi_2^{(\pm)} = \frac{2g}{4\epsilon^2 - \omega_{\sigma z}^2} \sigma^{(\pm)}, \quad (3.12b)$$

$$\sigma^{(\pm)} = \frac{1}{\sqrt{2\Omega} |\omega_{\sigma z}|} \frac{1}{\sqrt{\frac{1}{\lambda} - \frac{8\xi g^2}{\Omega} \sum_p' \frac{p^2}{\epsilon(4\epsilon^2 - \omega_{\sigma z}^2)^2}}}, \quad (3.12c)$$

$$\Pi_{\sigma}^{(\pm)} = \pm \frac{i\omega_{\sigma z}}{\lambda} \sigma^{(\pm)}. \quad (3.12d)$$

The modes are normalized according to

$$i\Omega \left(\sigma^{(\pm)} \Pi_{\sigma}^{(\pm)*} - \sigma^{(\pm)*} \Pi_{\sigma}^{(\pm)} - \frac{4\xi M^*}{\Omega} \sum_p' \frac{p^2}{\epsilon} (\Phi_1^{(\pm)} \Phi_2^{(\pm)*} - \Phi_1^{(\pm)*} \Phi_2^{(\pm)}) \right) = \pm \frac{\omega_{\sigma z}}{|\omega_{\sigma z}|}. \quad (3.13)$$

We turn now to the description of the pseudoscalar excitation. Its generator is given by eq. (3.6) and a dispersion relation can be obtained in a similar way as in the case of the scalar mode (note, however that the parameter λ has already been fixed). We get

$$\omega_{\Psi}^2 = 2(M^{*2} - M^2) + \frac{\xi g^2 \omega_{\Psi}^2}{2\Omega} \sum_{p < \Lambda} \left(\frac{1}{\epsilon_0^2} - \frac{1}{\epsilon(\epsilon^2 - \omega_{\Psi}^2/4)} \right) + \frac{2\xi g^2}{\Omega} \sum_{p < P_F} \frac{\epsilon}{\epsilon^2 - \omega_{\Psi}^2/4}. \quad (3.14)$$

For values of the Fermi momentum P_F such that $P_F < P_{FC}$ the above equation has one collective low-energy solution $\omega_{\Psi} = 0$. This solution corresponds to the pseudoscalar Goldstone boson. For $P_F \geq P_{FC}$ the chiral symmetry is restored and the scalar meson and pion masses are degenerate as expected. This result is also displayed in Fig. 3.

In order to generate normalizable RPA like states of the pionic excitation it is necessary to eliminate zero-valued frequencies. The solution to this problem is to introduce a perturbative term in the hamiltonian eq.(2.1) which explicitly breaks the chiral symmetry. This term is simply

$$\Omega \sigma c. \quad (3.15)$$

This term will not have any influence on the equilibrium value of the $\bar{\Psi}$ field, but now the expectation value of the scalar field in the vacuum will be given by

$$M^* = M = g\sigma_0 + \frac{c}{4g\sigma_0^2}, \quad (3.16)$$

as a consequence it appears an extra c/σ_0 term in the r.h.s. of eq.(3.14). This term is responsible for the existence of the pion mass in the vacuum ($P_F = 0$), and to get $\omega_{\Psi} = 138 \text{ MeV}$ we need $\sqrt{c/\sigma_0} = 140 \text{ MeV}$ for the values of M and g used in the figures. The presence of this new term (eq.(3.15)) in the hamiltonian has also the consequence of removing the degeneracy in the scalar and

pseudoscalar spectrum as is shown in Fig. 4. Again a comparison of the present results to those obtained in the context of the NJL model (refs. [13,14]) indicates that very similar predictions come out from both models for these parts of their mesonic sectors.

Again we have two discrete solutions of eq.(3.14), $\omega_{\Psi} = \pm\omega_{\pi}$, and the pseudoscalar RPA eigenmodes are given by

$$\bar{\Psi}^{(\pm)} = \frac{\bar{n}}{\sqrt{2\Omega} |\omega_{\pi}|} \frac{1}{\sqrt{\frac{1}{\lambda} - \frac{8\xi g^2}{\Omega} \sum_p' \frac{\epsilon}{(4\epsilon^2 - \omega_{\pi}^2)^2}}}, \quad (3.17a)$$

$$\bar{\Pi}_{\Psi}^{(\pm)} = \pm \frac{i\omega_{\pi}}{\lambda} \bar{\Psi}^{(\pm)}, \quad (3.17b)$$

$$\bar{S}_1^{(\pm)} = \pm \frac{ig\omega_{\pi}}{4\epsilon^2 - \omega_{\pi}^2} \bar{\Psi}^{(\pm)}, \quad (3.17c)$$

$$\bar{S}_2^{(\pm)} = \frac{2g\epsilon^2}{M^*} \frac{\bar{\Psi}^{(\pm)}}{4\epsilon^2 - \omega_{\pi}^2}, \quad (3.17d)$$

\bar{n} being an arbitrary unit isovector. These modes are normalized according to

$$i\Omega (\bar{\Psi}^{(\pm)} \bar{\Pi}_{\Psi}^{(\pm)*} - \bar{\Psi}^{(\pm)*} \bar{\Pi}_{\Psi}^{(\pm)} + \frac{4\xi M^*}{\Omega} \sum_p' \frac{1}{\epsilon} (\bar{S}_2^{(\pm)*} \bar{S}_1^{(\pm)} - \bar{S}_2^{(\pm)} \bar{S}_1^{(\pm)*})) = \pm \frac{\omega_{\pi}}{|\omega_{\pi}|}. \quad (3.18)$$

We are now in a position to calculate the pion decay constant by using the above presented eigenmodes. This is done following a very simple and commonly used procedure in nuclear structure calculations, which is well suited for the calculation of such a quantity. The pion decay constant is defined by the pion to vacuum transition amplitude induced by axial charges [20]

$$\langle 0 | Q_5^j | \Pi^k \rangle = i \sqrt{\frac{\Omega \omega_{\pi}}{2}} f_{\pi} \delta_{kj}, \quad (3.19)$$

where Q_5^j are the charge operators related to the time component of the axial current:

$$\bar{Q}_5 = \sum_{j=1}^N \gamma_5(j) \frac{\bar{\Psi}(j)}{2} + \int d^3x \frac{M^*}{g} \bar{\Pi}_{\Psi}, \quad (3.20)$$

for a static scalar field.

In our description the fields $\bar{\Pi}_{\Psi}, \bar{\Psi}$ are classical fields. The generator $\bar{\Pi}_{\Psi}$ being canonically conjugate to $\bar{\Psi}$ is to be understood as the generator for a fluctuation of the $\bar{\Psi}$ field. The axial charges are therefore associated with a special form of the generator eq.(3.6) given by

$$S_{2i}^{(j)} = \frac{1}{2} \delta_{ij}, \quad (3.21a)$$

$$\bar{S}_1 = 0, \quad (3.21b)$$

and $\bar{\Psi}, \bar{\Pi}_\psi$ fields given by

$$\Psi_i^{(j)} = \frac{M^*}{g} \delta_{ij}, \quad (3.21c)$$

$$\bar{\Pi}_\psi = 0, \quad (3.21d)$$

where j is associated with the component j of the axial charges (eq.(3.20)).

Such a state may be expanded in our normal RPA modes according to

$$\begin{pmatrix} M^*/g \\ 0 \\ 0 \\ 1/2 \end{pmatrix} = c_+ \begin{pmatrix} \Psi_i^{(+)} \\ \Pi_i^{(+)} \\ S_{1j}^{(+)} \\ S_{2j}^{(+)} \end{pmatrix} + c_- \begin{pmatrix} \Psi_i^{(-)} \\ \Pi_i^{(-)} \\ S_{1j}^{(-)} \\ S_{2j}^{(-)} \end{pmatrix}. \quad (3.22)$$

The signs + and - are related with positive and negative frequencies respectively, and $c_- = c_+^*$.

Using eq. (3.18) we can write the coefficient c_+ as

$$c_+ = \sqrt{\frac{\Omega |\omega_\pi|}{2}} \frac{M^*/g}{\sqrt{\frac{1}{\lambda} - \frac{8\xi g^2}{\Omega} \sum_p \frac{1}{(4\epsilon^2 - \omega_p^2)^2}}} \left(\frac{1}{\lambda} - \frac{2\xi g^2}{\Omega} \sum_p \frac{1}{\epsilon(4\epsilon^2 - \omega_p^2)} \right). \quad (3.23)$$

This coefficient can be interpreted as follows

$$c_+^* = -i \langle 0 | Q_5^j | \Pi^j \rangle = \sqrt{\frac{\Omega \omega_\pi}{2}} f_\pi. \quad (3.24)$$

This yields the following expression for the pion decay constant (in the bound state we have

$\omega_\pi \ll 2\epsilon$)

$$f_\pi = \frac{M^*}{g} \sqrt{\frac{1}{\lambda} - \frac{\xi g^2}{2\Omega} \sum_p \frac{1}{\epsilon^3}}. \quad (3.25)$$

In the vacuum, and using eq. (3.10)

$$f_\pi = \frac{M}{g}, \quad (3.26)$$

holds exactly. Equation (3.26) agrees with the Goldberger-Treiman relation. In order to reproduce the experimental pion decay constant, for instance $f_\pi = 93 \text{ MeV}$, for a constituent quark mass $M_{u,d} = 320 \text{ MeV}$ we get for the coupling constant $g = 3.44$. These were the values used in all numerical calculations.

4. PSEUDOSCALAR MESON SPECTRA IN THE CONTINUUM

In order to study the RPA normal modes in the continuum it is convenient to write the Lagrangian eq.(3.2) in a dimensionless form. Inserting eq.(3.6) in eq.(3.2), and using the dimensionless quantities

$$\bar{Q} = \delta \bar{\Psi} / M, \quad (4.1a)$$

$$\bar{P} = \bar{\Pi}_\psi / M^2 = \delta \bar{\Psi} / \lambda M^2, \quad (4.1b)$$

$$x = \epsilon^2 / M^2, \quad (4.1c)$$

$$m = M^* / M, \quad (4.1d)$$

$$f(x) = \frac{\xi}{2\pi^2} \sqrt{\frac{x-m^2}{x}}. \quad (4.1e)$$

$$4\alpha^2 = 2(m^2 - 1 + \frac{c}{2\sigma_0 M^2}) + g^2 \int_{m^2}^{x_A} dx f(x). \quad (4.1f)$$

we get

$$\begin{aligned} \frac{L_\psi}{M^4 \Omega} = & \frac{1}{2} (\bar{P}^* \dot{\bar{Q}} - \dot{\bar{P}} \bar{Q}^*) - m \int_{x_F}^{x_A} dx f(x) (\bar{S}_2^* \dot{\bar{S}}_1 - \dot{\bar{S}}_1^* \bar{S}_2) - 2 \int_{x_F}^{x_A} dx f(x) (m^2 |\bar{S}_2|^2 + |\bar{S}_1|^2) \\ & + gm \bar{Q}^* \int_{x_F}^{x_A} dx f(x) \bar{S}_2 + gm \bar{Q} \int_{x_F}^{x_A} dx f(x) \bar{S}_2^* - \frac{1}{2} (\lambda |\bar{P}|^2 + 4\alpha^2 |\bar{Q}|^2) \end{aligned} \quad (4.2)$$

where all time derivatives are related to $\tau = Mt$.

The Euler-Lagrange equations are

$$\ddot{\bar{Q}} - \lambda \bar{P} = 0, \quad (4.3a)$$

$$\ddot{\bar{P}} + 4\alpha^2 \bar{Q} - 2mg \int_{x_F}^{x_A} dx f(x) \bar{S}_2(x) = 0, \quad (4.3b)$$

$$m \ddot{\bar{S}}_2(x) - 2x \bar{S}_1(x) = 0, \quad (4.3c)$$

$$\ddot{\bar{S}}_1(x) - g \bar{Q} + 2m \bar{S}_2(x) = 0, \quad (4.3d)$$

and using the ansatz

$$\begin{bmatrix} \bar{Q}(\tau) \\ \bar{P}(\tau) \\ \bar{S}_1(x, \tau) \\ \bar{S}_2(x, \tau) \end{bmatrix} = \begin{bmatrix} \bar{Q}_\omega \\ \bar{P}_\omega \\ \bar{S}_{1\omega}(x) \\ \bar{S}_{2\omega}(x) \end{bmatrix} e^{i\omega\tau} \quad (4.4)$$

we get the following equations to the normal modes

$$i\omega\bar{Q}_\omega = \lambda\bar{P}_\omega, \quad (4.5a)$$

$$i\omega\bar{P}_\omega = -4\alpha^2\bar{Q}_\omega + 2mg \int_{x_F}^{x_A} dx f(x)\bar{S}_{2\omega}(x), \quad (4.5b)$$

$$i\omega\bar{S}_{1\omega}(x) = g\bar{Q}_\omega - 2m\bar{S}_{2\omega}(x), \quad (4.5c)$$

$$i\omega\bar{S}_{2\omega}(x) = \frac{2x}{m}\bar{S}_{1\omega}(x). \quad (4.5d)$$

As mentioned before, there are always two types of solutions of eqs. (4.5). Two discrete modes, $\omega = \pm\omega_z$, if $\omega_z^2 < 4x_F$ (the subscript z denoting "zero-sound" values) and a continuum of solutions if $4x_F < \omega^2 < 4x_A$.

The dispersion relation for "zero-sound" solutions is

$$\frac{\omega_z^2}{4\lambda} - \alpha^2 + \frac{g^2}{4} \int_{x_F}^{x_A} dx f(x) \frac{x}{x - \omega_z^2/4} = 0 \quad (4.6)$$

and the discrete modes are described by

$$\bar{Q}_\pm = \bar{n}, \quad (4.7a)$$

$$\bar{P}_\pm = \pm \frac{i\omega_z}{\lambda} \bar{n}, \quad (4.7b)$$

$$\bar{S}_{1\pm}(x) = \pm \frac{i\omega_z g}{4} \frac{\bar{n}}{x - \omega_z^2/4}, \quad (4.7c)$$

$$\bar{S}_{2\pm}(x) = \frac{gx}{2m} \frac{\bar{n}}{x - \omega_z^2/4}, \quad (4.7d)$$

the only difference with eqs.(3.17) being the fact that now the modes are not normalized. In the continuum the normal modes are given by

$$\bar{Q}_\omega = -\frac{2m}{g} a(\omega^2/4) \bar{n}, \quad (4.8a)$$

$$\bar{P}_\omega = -\frac{i\omega 2m}{\lambda g} a(\omega^2/4) \bar{n}, \quad (4.8b)$$

$$\bar{S}_{1\omega}(x) = i\omega \frac{m}{2x} \bar{S}_{2\omega}(x), \quad (4.8c)$$

$$\bar{S}_{2\omega}(x) = \left(\delta(\omega^2/4 - x) + \frac{xa(\omega^2/4)}{\omega^2/4 - x} \right) \bar{n}, \quad (4.8d)$$

where $a(\omega^2/4)$ satisfies the equation

$$a(\omega^2/4) = \frac{g^2 f(\omega^2/4)}{\omega^2/\lambda - 4\alpha^2 + g^2 \int_{x_F}^{x_A} dx f(x) \frac{x}{x - \omega^2/4}}. \quad (4.9)$$

In what follows and in eq.(4.9), integrals involving the factor $1/(x - \omega^2/4)$ have to be interpreted as principal value integrals.

It can be seen from eqs.(4.5) that the normal modes are orthogonal, and using eqs.(4.7) and (4.8) we get the following orthogonality relations:

$$i \left(\bar{P}_\omega^* \bar{Q}_\omega - \bar{Q}_\omega^* \bar{P}_\omega - 2m \int_{x_F}^{x_A} dx f(x) (\bar{S}_{2\omega}^* \bar{S}_{1\omega} - \bar{S}_{1\omega}^* \bar{S}_{2\omega}) \right) = m^2 \frac{f(\omega^2/4)}{\omega^2/4} \delta(\omega/2 - \omega'/2), \quad (4.10a)$$

$$i \left(\bar{Q}_\pm \bar{P}_\omega^* - \bar{P}_\omega \bar{Q}_\pm^* - 2m \int_{x_F}^{x_A} dx f(x) (\bar{S}_{1\pm} \bar{S}_{2\omega}^* - \bar{S}_{2\pm} \bar{S}_{1\omega}^*) \right) = 0, \quad (4.10b)$$

$$i \left(\bar{Q}_\pm \bar{P}_\pm^* - \bar{P}_\pm \bar{Q}_\pm^* - 2m \int_{x_F}^{x_A} dx f(x) (\bar{S}_{1\pm} \bar{S}_{2\pm}^* - \bar{S}_{2\pm} \bar{S}_{1\pm}^*) \right) = \pm \eta, \quad (4.10c)$$

where

$$\eta = 2\omega_z \left(\frac{1}{\lambda} + \frac{g^2}{4} \int_{x_F}^{x_A} dx f(x) \frac{x}{(x - \omega_z^2/4)^2} \right). \quad (4.11)$$

It has been shown by van Kampem [21], for the electron plasma, and in ref.[22] for the nuclear case, that this set of solutions is complete. This means that given an arbitrary initial state

$$\Psi_0 = \begin{bmatrix} \bar{Q}_0(0) \\ \bar{P}_0(0) \\ \bar{S}_1(x, 0) \\ \bar{S}_2(x, 0) \end{bmatrix} = \begin{bmatrix} \bar{Q}_0 \\ \bar{P}_0 \\ \bar{H}_1(x) \\ \bar{H}_2(x) \end{bmatrix} \quad (4.12)$$

there is a function $c(\omega)$ and numbers C_+, C_- such that

$$\begin{bmatrix} \bar{Q}_0 \\ \bar{P}_0 \\ \bar{H}_1(x) \\ \bar{H}_2(x) \end{bmatrix} = \int_{2\sqrt{x_F}}^{2\sqrt{x_A}} c(\omega) \begin{bmatrix} \bar{Q}_\omega \\ \bar{P}_\omega \\ \bar{S}_{1\omega}(x) \\ \bar{S}_{2\omega}(x) \end{bmatrix} d\omega + C_+ \begin{bmatrix} \bar{Q}_+ \\ \bar{P}_+ \\ \bar{S}_{1+}(x) \\ \bar{S}_{2+}(x) \end{bmatrix} + C_- \begin{bmatrix} \bar{Q}_- \\ \bar{P}_- \\ \bar{S}_{1-}(x) \\ \bar{S}_{2-}(x) \end{bmatrix} \quad (4.13)$$

Following van Kampen [21] and making use of the auxiliary functions

$$F_\pm(\omega^2/4) = \frac{g^2}{2\pi i(\omega^2/\lambda - 4\alpha^2)} \int_{x_F}^{x_A} dx \frac{xf(x)}{x - \omega^2/4 \pm i\delta}, \quad (4.14a)$$

$$\bar{G}_{1\pm} = \frac{g^2}{2\pi i(\omega^2/\lambda - 4\alpha^2)} \left(\int_{x_F}^{x_A} dx \frac{x f(x) \bar{H}_1(x)}{x - \omega^2/4 \pm i\delta} + \bar{A}_1 \right), \quad (4.14b)$$

$$\bar{G}_{2\pm} = \frac{g^2}{2\pi i(\omega^2/\lambda - 4\alpha^2)} \left(\int_{x_F}^{x_A} dx \frac{f(x) \bar{H}_2(x)}{x - \omega^2/4 \pm i\delta} + \bar{A}_2 \right), \quad (4.14c)$$

and

$$\bar{K}_{j\pm}(\omega^2/4) = \frac{\bar{G}_{j\pm}(\omega^2/4)}{1 + 2\pi i F_{\pm}(\omega^2/4)}, \quad (4.14d)$$

where \bar{A}_1, \bar{A}_2 are constants to be determined by the initial values \bar{P}_0 and \bar{Q}_0 respectively, and δ is an infinitesimal, we can show that

$$c(\omega) = \frac{\bar{n}}{2\alpha(\omega^2/4)} \left(\frac{-i}{m} (\bar{K}_{1+}(\omega^2/4) - \bar{K}_{1-}(\omega^2/4)) + \frac{\omega}{2} (\bar{K}_{2+}(\omega^2/4) - \bar{K}_{2-}(\omega^2/4)) \right). \quad (4.15)$$

Using eqs.(4.14) and eq.(4.15) we finally get

$$c(\omega) = \frac{\bar{c}(\omega)}{1 + \pi^2 a^2 (\omega^2/4) \omega^2/4}, \quad (4.16)$$

$$\bar{c}(\omega) = \frac{i\omega^2/4}{4m^2 f(\omega^2/4)} \left(\bar{Q}_0 \bar{P}_\omega^* - \bar{P}_0 \bar{Q}_\omega^* - 2m \int_{x_F}^{x_A} dx f(x) (\bar{H}_1(x) \bar{S}_{2\omega}^*(x) - \bar{H}_2(x) \bar{S}_{1\omega}^*(x)) \right). \quad (4.17)$$

where we have already used the solutions $\bar{A}_1 = \bar{P}_0/g$ and $\bar{A}_2 = 2\bar{Q}_0/(mg\lambda)$.

One is not allowed to use the orthogonality relations to derive $c(\omega)$ because of the singularities in $\bar{S}_{1\omega}(x)$ and $\bar{S}_{2\omega}(x)$, but we can obtain the expressions to C_{\pm} directly from these equations. It gives

$$C_{\pm} = \pm \frac{i}{\eta} \left(\bar{P}_{\pm}^* \bar{Q}_0 - \bar{Q}_{\pm}^* \bar{P}_0 - 2m \int_{x_F}^{x_A} dx f(x) (\bar{H}_1(x) \bar{S}_{2\pm}^*(x) - \bar{H}_2(x) \bar{S}_{1\pm}^*(x)) \right), \quad (4.18)$$

The solution of the initial value problem satisfying both eq.(4.3) and the initial condition eq.(4.12)

is therefore

$$\begin{bmatrix} \bar{Q}(\tau) \\ \bar{P}(\tau) \\ \bar{S}_1(x, \tau) \\ \bar{S}_2(x, \tau) \end{bmatrix} = \int_{2\sqrt{x_F}}^{2\sqrt{x_A}} c(\omega) \begin{bmatrix} \bar{Q}_\omega \\ \bar{P}_\omega \\ \bar{S}_{1\omega}(x) \\ \bar{S}_{2\omega}(x) \end{bmatrix} e^{i\omega\tau} d\omega + C_+ \begin{bmatrix} \bar{Q}_+ \\ \bar{P}_+ \\ \bar{S}_{1+}(x) \\ \bar{S}_{2+}(x) \end{bmatrix} e^{i\omega_+ \tau} + C_- \begin{bmatrix} \bar{Q}_- \\ \bar{P}_- \\ \bar{S}_{1-}(x) \\ \bar{S}_{2-}(x) \end{bmatrix} e^{-i\omega_- \tau}. \quad (4.19)$$

The use of sum rules is a complementary approach to the use of equations of motion when one is looking at collective states microscopically. Following ref.[19], we find that the amplitudes $\bar{c}(\omega), C_+$

and C_- satisfy the energy weighted sum rule (EWSR):

$$4m^2 \int_{2\sqrt{x_F}}^{2\sqrt{x_A}} d\omega \frac{|\bar{c}(\omega)|^2 f(\omega^2/4)}{\omega/2(1 + \pi^2 a^2 (\omega^2/4) \omega^2/4)} + \frac{\omega_z}{2} \eta (|C_+|^2 + |C_-|^2) = \frac{1}{2} (\lambda |\bar{P}_0|^2 + 4\alpha^2 |\bar{Q}_0|^2) + 2 \int_{x_F}^{x_A} dx f(x) (m^2 |\bar{H}_2|^2 + x |\bar{H}_1|^2) - gm \bar{Q}_0 \cdot \int_{x_F}^{x_A} dx f(x) \bar{H}_2^*(x) - gm \bar{Q}_0^* \cdot \int_{x_F}^{x_A} dx f(x) \bar{H}_2(x). \quad (4.20)$$

The strength function representing the pionic mode in the $q\bar{q}$ continuum is

$$s_\pi(\omega) = \frac{4m^2 |\bar{c}(\omega)|^2 f(\omega^2/4)}{\omega/2(1 + \pi^2 a^2 (\omega^2/4) \omega^2/4)}. \quad (4.21)$$

The simplest example of initial condition which favours the mode in the continuum is [23]

$$\Psi_0 = \begin{bmatrix} 0 \\ 0 \\ 0 \\ \bar{n} \end{bmatrix} \quad (4.22)$$

for this condition, the strength function in the vacuum ($P_F = 0, m = 1$) becomes

$$s_\pi(\omega) = \frac{\omega/2 f(\omega^2/4) (m_\pi/2M)^4}{\left(\frac{g^2}{4} \frac{\omega^2}{4} \int_{x_F}^{x_A} dx \frac{f(x)}{\omega^2/4 - x} + \left(\frac{m_\pi}{2M} \right)^2 - \frac{\omega^2}{4\lambda} \right)^2 + \pi^2 \frac{g^4}{16} \frac{\omega^2}{4} f(\omega^2/4)} \quad (4.23)$$

and, from eq.(4.20) the EWSR is

$$m_1 = 2 \int_1^{x_A} dx f(x). \quad (4.24)$$

The fraction of the EWSR exhausted by the discrete frequency $\pm\omega_z$, in this case, is

$$F(\omega_z) = \frac{4\omega_z^2}{\eta g^2} \left(\left(\frac{m_\pi}{M\omega_z} \right)^2 - \frac{1}{\lambda} \right)^2 \frac{1}{m_1}, \quad (4.25)$$

with ω_z given by eq. (4.4) that we can rewrite as

$$\omega_z^2 \left(\frac{1}{\lambda} + \frac{g^2}{4} \int_1^{x_A} dx \frac{f(x)}{x - \omega_z^2/4} \right) = \left(\frac{c}{\sigma_0 M} \right)^2. \quad (4.26)$$

In spite of both c/σ_0 and the maximum in $s(\omega)$ being independent of Λ in the limit $\Lambda \rightarrow \infty$, the EWSR is not satisfied if $\Lambda \geq 2.018M(1/\lambda \leq 0)$. It is because, as pointed out in ref.[16], one imaginary solution of eq.(4.6) appears if $1/\lambda < 0$, and in this case the set of solutions eqs.(4.7) and (4.8) is not complete. From this imaginary solution we should not infer that the minimum of the

potential energy eq.(2.7) is a local minimum only. The imaginary solution reflects, instead, the fact that the kinetic energy controlling the scalar meson field dynamics became negative.

This imaginary solution corresponds to the Perry's instability momentum, and can be avoid if the cutoff is kept finite ($\Lambda < 2.018M$). The only consequence of working with a finite cutoff is the fact that we have to interpret the theory as some sort of effective theory useful for a restricted class of calculation, as suggested by Cohen et al.[7].

Our EWSR can also provide a tool to investigate the importance of the instability. If, for some value of the cutoff, the EWSR is not strongly violated, we can say that the existence of the instability is not infecting the calculations and the simplest procedure, in this case, is to ignore the problem [24], as suggested by Perry.

To the initial condition eq.(4.22) we found that the EWSR is minimally violated (less than 1.5%) for $\Lambda/M = 15$. Fig.5 shows the strength function eq.(4.23) calculated with this value of Λ . It exhibits a pronounced maximum around 2200 MeV which is of the same order of the experimental mass of the (not well established) resonance $\pi(1300)$ [25], which is indicated by an arrow. For this initial condition, 98.2% of the total EWSR lies in the continuum while only 0.5% is exhausted by the discrete frequencies.

On the other hand, if we want to avoid the imaginary solution we must have $\Lambda < 2.018M$, and, in this situation, two new discrete modes will appear with $\omega = \pm\omega_>, \omega_>^2 > 4x_\Lambda$. The fraction of the EWSR exhausted by these new modes is also given by eq.(4.25), the only difference with the "zero-sound" values being the value of ω . In Fig.6 the strength function eq.(4.23) calculated with $\Lambda = 2.017M$ is shown. The maximum is not so pronounced as in Fig.5 and it is around 1100 MeV. An arrow indicates the experimental value.

To this value of Λ almost the EWSR is exhausted by these new modes $\pm\omega_>$ which numerical solution is $\omega_> = 48,340 MeV$. We see that this solution has no physical significance since do not exist mesons, with the same quantum numbers of the pion, with this mass.

5. SUMMARY AND CONCLUSIONS

In the present work we consider a chiral lagrangian consisting of a fermionic field coupled to scalar and pseudoscalar meson fields. The description treats the fermions quantum-mechanically and the

meson fields classically. The effects of the Dirac sea is properly included. By means of traditional many body techniques we obtain a set of stationary modes of small amplitude excitation (which includes the continuum in a natural way) satisfying orthogonality and completeness relations. The corresponding EWSR is also obtained and shown to provide for a very useful tool to investigate the importance of the instabilities that always appear for all nonasymptotically free theories, at the one-loop level (equivalent to RPA) calculations. These instabilities are usually found in the literature and, to our knowledge, it is the first time a quantitative analysis of its importance is given.

Moreover, exploring the bosonic sector of the linear σ model with the above method shows that our results are in excellent agreement with the ones found for light mesons in the NJL model. This indicates that the linear chiral σ model is well suited to provide for a unified description of both, baryonic and light meson properties

REFERENCES

- 1) E. Witten, Nucl.Phys. B160(1979)57.
- 2) D. Dyakonov and Yu.V. Petrov, Nucl. Phys. B272 (1986) 457.
- 3) D. MacKay and H. Munczek, Phys. Rev. D32 (1985) 266.
- 4) P. Simic, Phys. Rev. D34 (1986) 1903.
- 5) R. Cahill and C. Roberts, Phys. Rev. D32 (1985) 2419.
- 6) A. Adrianov, Phys. Lett. 157B (1985) 425.
- 7) R.J. Perry, Phys. Lett. B199 (1987) 489; T.D. Cohen, M.K. Banerjee and C-Y. Ren, Phys. Rev. C36 (1987) 1653.
- 8) A. Chodos, R.L. Jaffe, K. Johnson, C.B. Thorn and V.F. Weisskopf, Phys. Rev. D9 (1974) 3471; A. Chodos, R.L. Jaffe, K. Johnson and C.B. Thorn, Phys. Rev. D10 (1974) 2599.
- 9) G.A. Miller, A.W. Thomas and S. Théberge, Phys. Lett. 91B (1980) 192; A.W. Thomas in Advances in Nuclear Physics, edited by J. Negele and E. Vogt (Plenum, New York, 1983) vol.13.
- 10) G.S. Adkins, C.R. Nappi and E. Witten, Nucl. Phys. B228 (1983) 552; G.S. Adkins and C.R. Nappi, Phys. Lett. 137B (1984) 251.
- 11) Y. Nambu and G. Jona-Lasinio, Phys. Rev. 122 (1961) 354.
- 12) V. Bernard, R. Brockmann, M. Schaden, W. Weise and E. Werner, Nucl. Phys. A412(1984)349.
- 13) J. da Providência, M.C. Ruivo, C.A. de Sousa, Phys. Rev. D36 (1987) 1282.
- 14) C.A. de Sousa, Z. Phys. C43(1989)503.
- 15) A. H. Blin, B. Hiller and J. da Providência, Phys.Lett. 241B (1990)1; J. da Providência and C. A. de Sousa, Phys. Lett. 237B(1990)147.
- 16) T. Kohmura, Y. Miyana, T. Nagai, S. Ohmaka, J. da Providência and T. Kodama, Phys. Lett. 226B(1989)207.
- 17) K. Ando, A. Ikeda and G. Holzwarth, Z. Phys. A310(1983)223.
- 18) M. Gell-Mann and M. Lévi, Nuovo Cimento 16 (1960) 705.
- 19) D. M. Brink and J. da Providência, Nucl. Phys. A500(1989)301.
- 20) W. Weise, International Review of Nuclear Physics, vol. 1, ed. W. Weise, chap. 2 (1984).
- 21) N. G. van Kampen, Physica 21 (1955) 949.
- 22) M. C. Nemes, A. F. R. T. Piza, and J. da Providência, Physica 146 A (1987) 282.
- 23) M. Nielsen and J. da Providência, Phys. Rev C40(1989)2377.
- 24) M.C. Nemes, M. Nielsen, M.M. de Oliveira and J. da Providência, to appear in Phys. Lett. B.
- 25) Particle Data Group: M. Aguilar-Benitez et al., Phys. Lett. 204B(1988)1.

FIGURE CAPTIONS

Fig.1- The energy per volume in homogeneous quark matter in units of M^4 (the vacuum quark mass) for different values of the Fermi momentum for the parameter values: $g = 3.44$ and $K = 2g^2$. The curves are in different scales so that details can be observed.

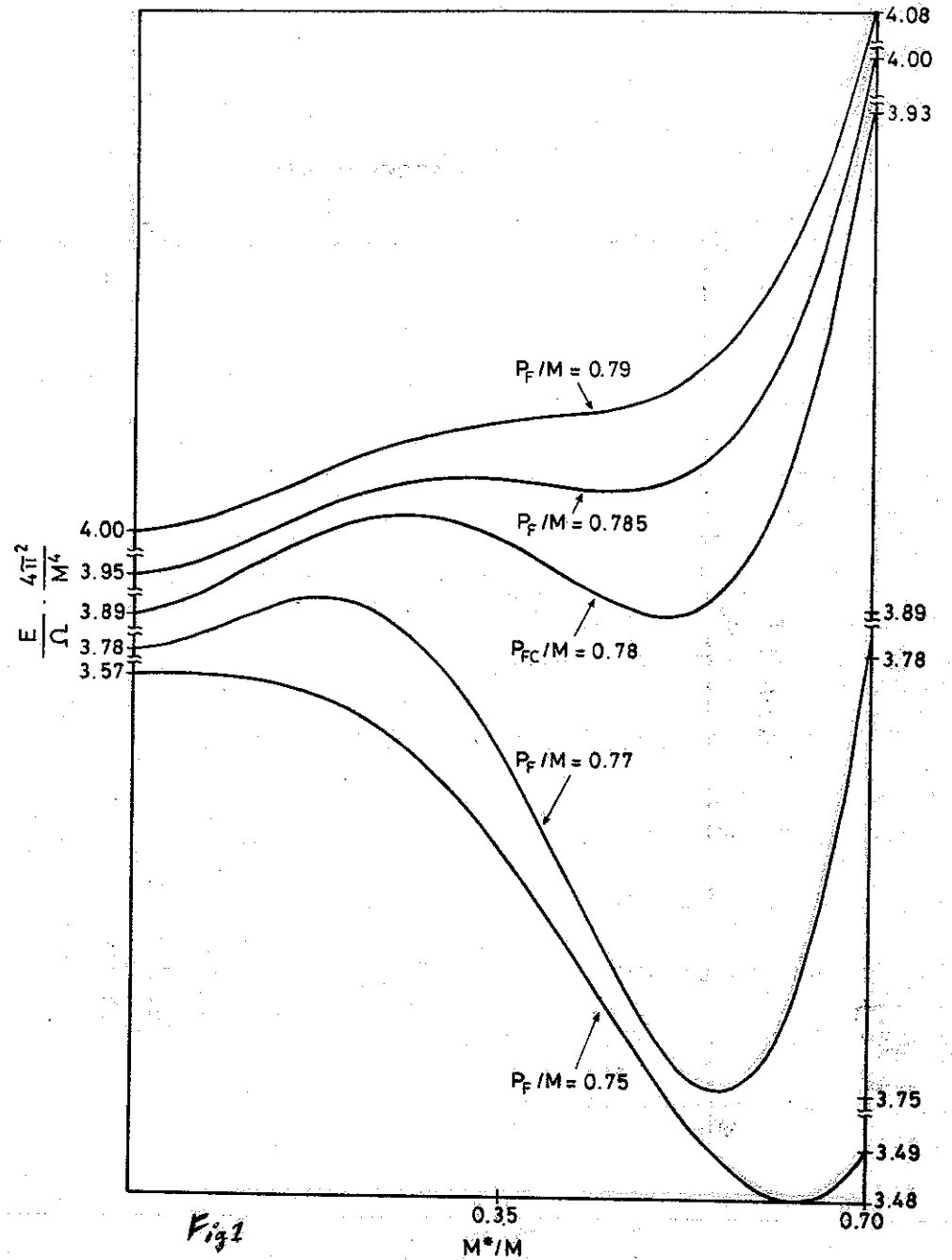
Fig.2- The energy per particle as a function of the Fermi momentum for the parameter values: $g = 3.44, K = 2g^2, M = 320MeV$.

Fig.3- The effective quark mass (dotted line), the scalar meson spectra (solid line) and the pseudoscalar meson spectra (dashed line) as a function of the Fermi momentum for the parameter values : $g = 3.44, K = 2g^2, M = 320MeV$. The point P_{FC} indicates the value of P_F for which the chiral symmetry is restored.

Fig.4- The pseudoscalar (solid line) and the scalar (dashed line) mesons spectra when the chiral symmetry is broken, for the parameter values : $g = 3.44, K = 2g^2, M = 320MeV, m = 142MeV$.

Fig.5- Strength function representing the pion resonance, as a function of ω for $\Lambda = 15M$. The arrow indicates the experimental mass.

Fig.6- Same as Fig.5 for $\Lambda = 2.017M$.



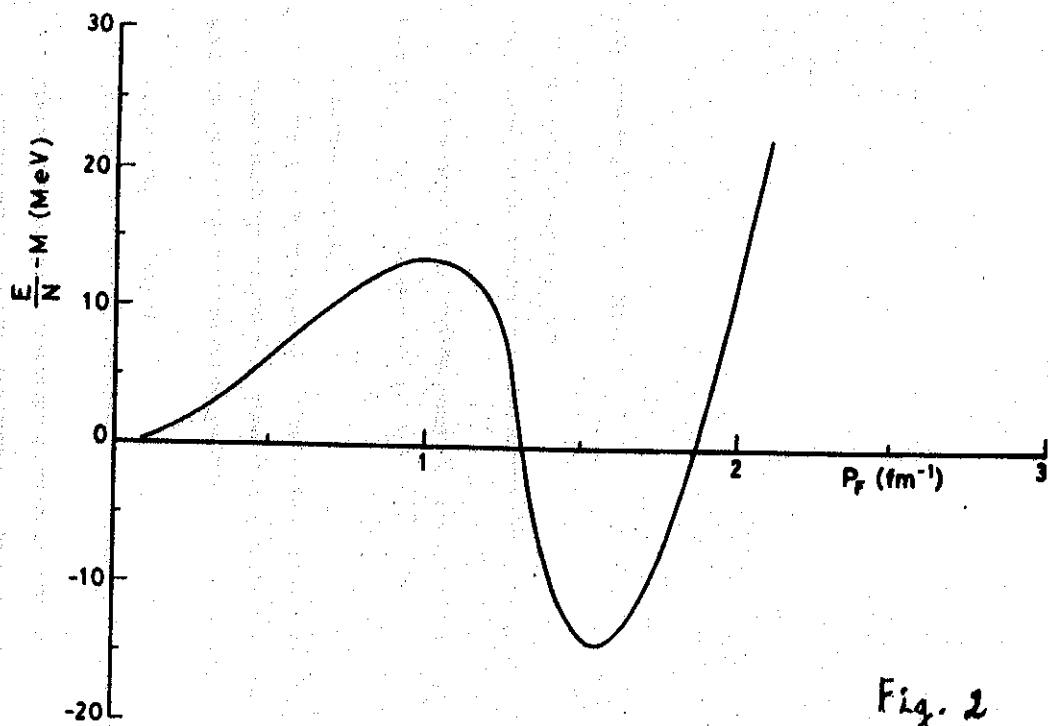


Fig. 2

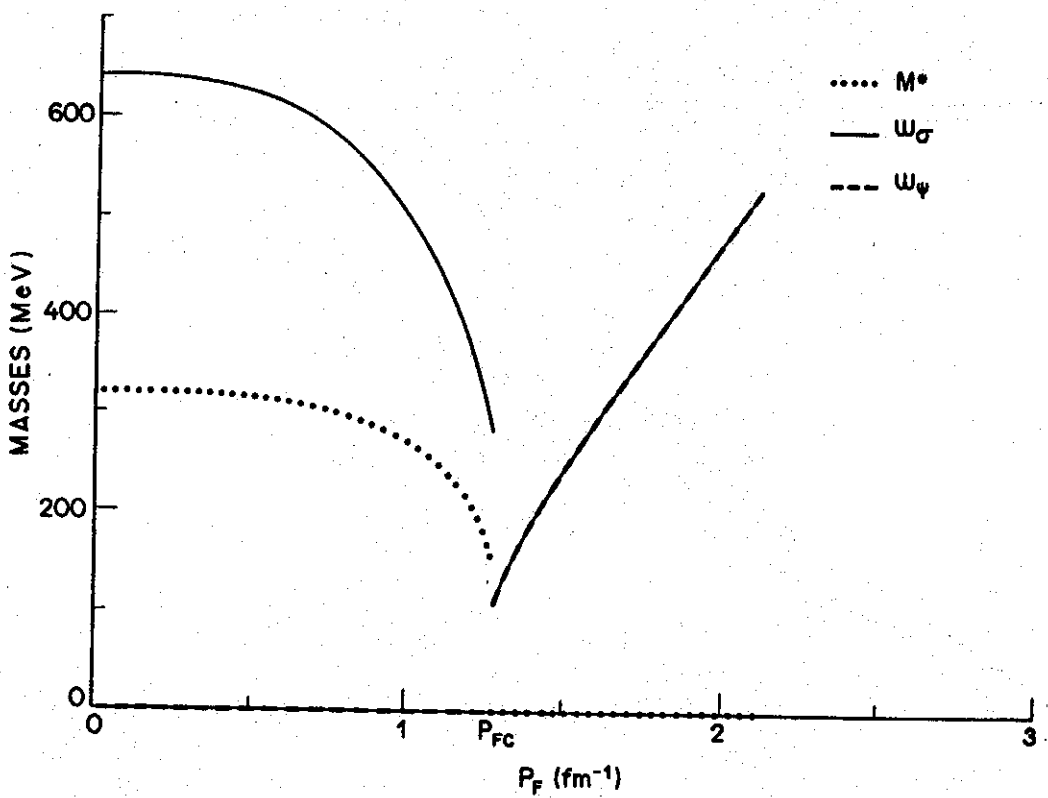


Fig. 3

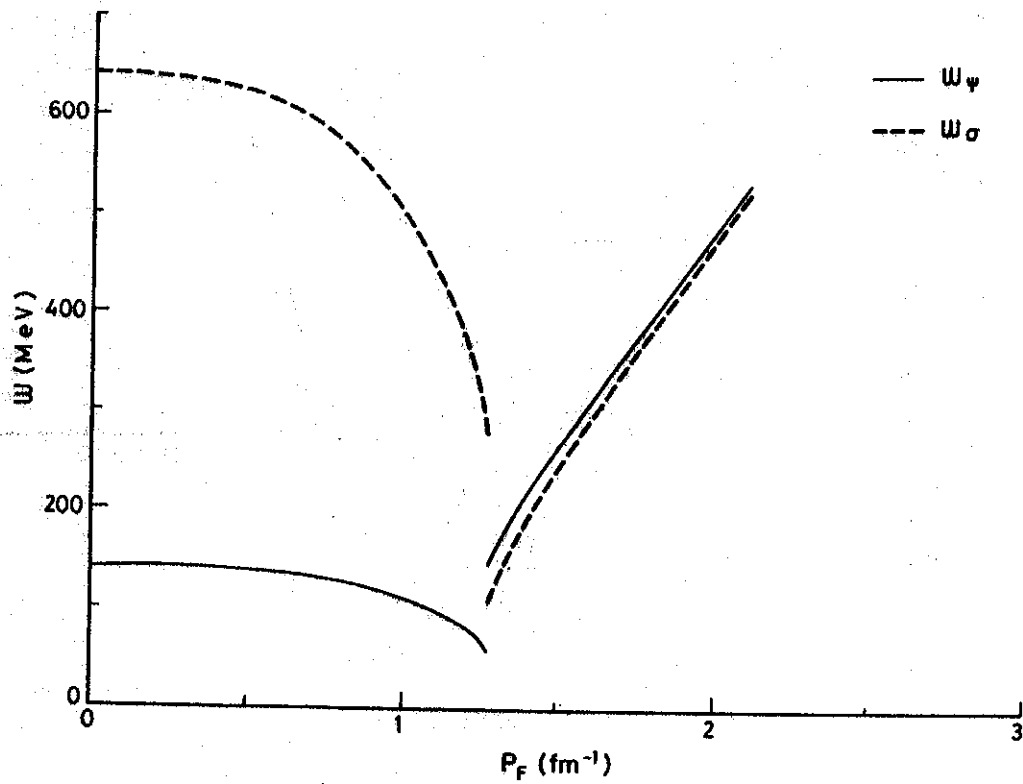


Fig. 4

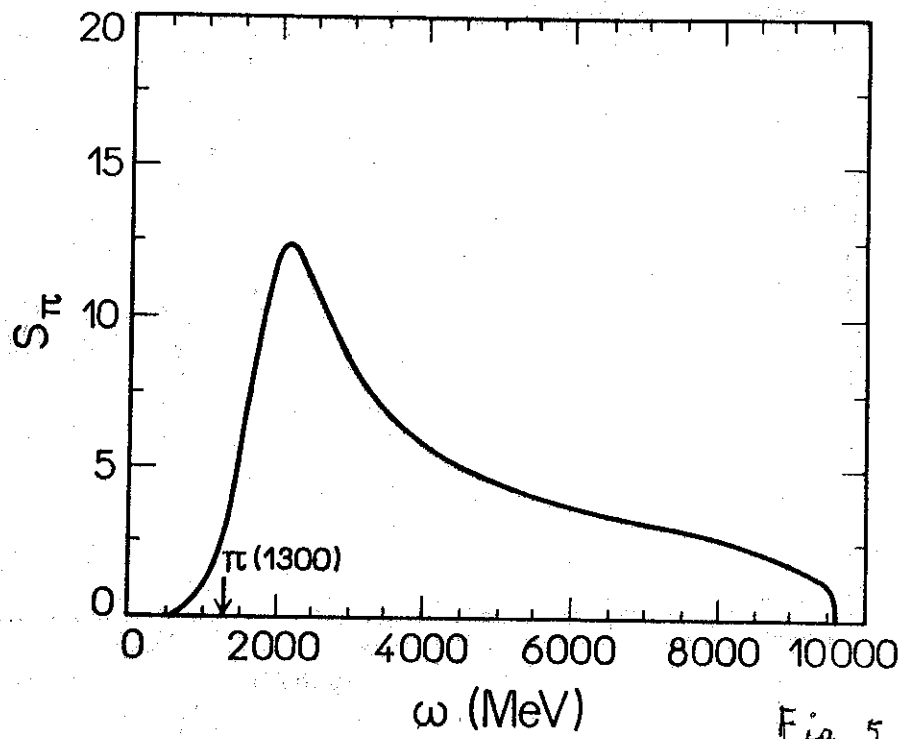


Fig. 5

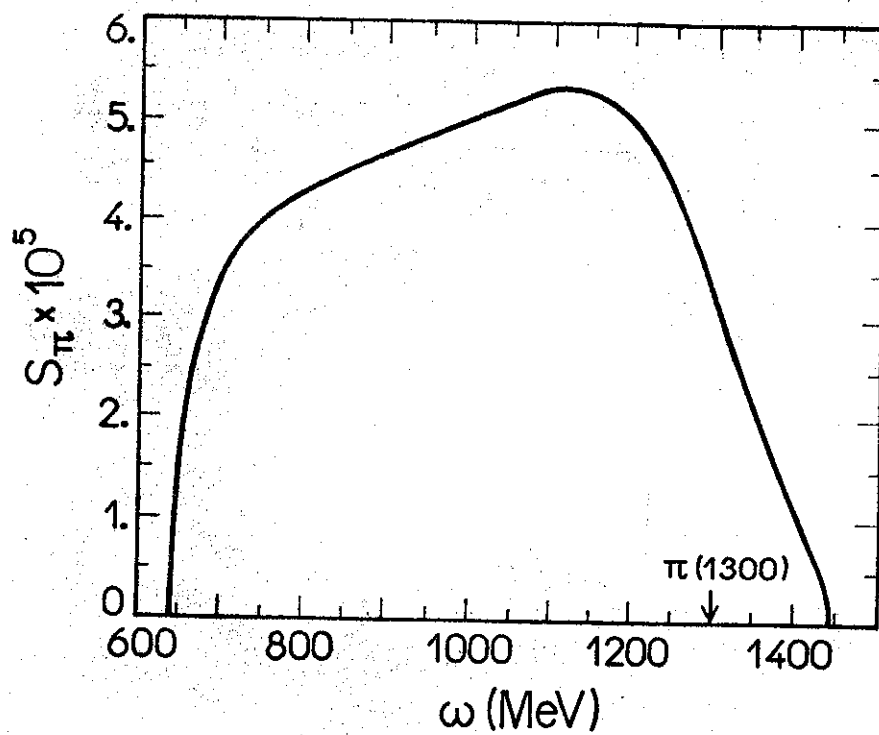


Fig. 6